Dimerization of hub protein DYNLL1 and bZIP transcription factor CREB3L1 enhances transcriptional activation of CREB3L1 target genes like arginine vasopressin

Mingkwan Greenwood[1], Benjamin T Gillard[1], David Murphy[1], Michael P Greenwood[1]*

1. Molecular Neuroendocrinology Research Group, Bristol Medical School: Translational Health Sciences, University of Bristol, Dorothy Hodgkin Building, Bristol, United Kingdom.

*Corresponding author – Michael Greenwood

Michael Greenwood
Dorothy Hodgkin Building
University of Bristol
Whitson Street
BS1 3NY

Email: mike.greenwood@bristol.ac.uk

Declarations of interest: none

Abstract

bZIP transcription factors can function as homodimers or heterodimers through interactions with their disordered coiled-coil domain. Such dimer assemblies are known to influence DNA-binding specificity and/or the recruitment of binding partners, which can cause a functional switch of a transcription factor from being an activator to a repressor. We recently identified the genomic targets of a bZIP transcription factor called CREB3L1 in rat hypothalamic supraoptic nucleus by ChIP-seq. The objective of this study was to investigate the CREB3L1 protein-to-protein interactome of which little is known. For this approach, we created and screened a rat supraoptic nucleus yeast two-hybrid prey library with the bZIP region of rat CREB3L1 as the bait. Our yeast two-hybrid approach captured five putative CREB3L1 interacting prey proteins in the supraoptic nucleus. One interactor was selected by bioinformatic analyses for more detailed investigation by co-immunoprecipitation, immunofluorescent cellular localisation, and reporter assays *in vitro*. Here we identify dimerisation hub protein Dynein Light Chain LC8-Type 1 as a CREB3L1 interacting protein that *in vitro* enhances CREB3L1 activation of target genes.

Keywords

Transcription; Transcription factor; Basic leucine zipper; Yeast two-hybrid; Supraoptic nucleus; Vasopressin.

1. Introduction

Transcription factor CREB3L1 (cAMP responsive element binding protein 3 like 1), also known as old astrocyte specifically induced substance (OASIS), was first identified in long-term cultured astrocytes and gliotic tissue (1). It is one of five members of the CREB3 basic leucine zipper domain transcription factor subfamily (also known as bZIP) that also includes CREB3 (also known as LUMAN), CREB3L2 (also known as BBF2H7), CREB3L3 (also known as CREBH) and CREB3L4 (also known as AIbZIP) (2). The CREB3 subfamily of transcription factors are structurally similar to activating transcription factor 6, a classical endoplasmic reticulum (ER) stress transducer, but are activated by a diverse range of stimuli in a cell-type specific manner (3). Upon stimulation, the CREB3 family of proteins are transported from the ER to Golgi complex where they are activated by regulated intramembrane proteolysis (RIP), first by site-1-protease (S1P), giving rise to an intermediate cleavage product, followed by site-2-protease (S2P) cleavage to liberate an N-terminal active fragment that can then translocate to the nucleus to activate the transcription of target genes by binding to specific cis-acting promoter sequences (4-6). CREB3L1 is expressed by several tissues, mostly secretory organs/cells, such as the pancreas, placenta, prostate gland, thyroid gland, gastrointestinal tract, osteocytes, cancer cells, and neuroendocrine cells of the hypothalamus (7, 8). Therefore, new knowledge of CREB3L1 functions is crucial for our understanding of many physiological processes and diseases.

To function normally, transcription factors must be selectively transported to their destinations where they can mediate their physiological functions. In the case of the CREB3 family members they are trafficked from the endoplasmic reticulum (ER) to Golgi, cleaved, then transported efficiently through the nuclear pore complex, which penetrates the nuclear envelope (9). Transport to the nucleus necessitates the presence of nuclear localisation signals or chaperone proteins that possess these signals. The bZIP proteins can function as homodimers and heterodimers through interactions with their disordered coiled-coil domain, and these dimer assemblies influence the DNA-binding specificity and affinity and/or the recruitment of different binding partners (10, 11). In some cases, this can cause a functional switch of a transcription factor from being an activator to a repressor of transcription. This ability vastly expands the DNA binding range of bZIP transcription factors with different combinations binding to different DNA motifs and subsequently altering different biological pathways in a stimulus dependent manner.

The expression of CREB3 family member CREB3L1 is synonymous with specialised secretory cell-types throughout the body, for examples osteoblasts, astrocytes, and hypothalamic neurones, all with high demands for protein synthesis and secretion (5, 6, 12-15). CREB3L1 regulates a wide array of cellular functions including roles in ER stress, hormone synthesis and secretion, the formation of the extracellular matrix, protein transport, cell organelle size, cell proliferation, and cell cycle control (16-20). Subsequently, CREB3L1 is activated by a diverse array of stimuli including ER stress, osmotic stimulation, and DNA damage. What is not well understood is how CREB3L1 is able to service such a large array of cellular functions. We reasoned that this may be supported by an equally diverse CREB3L1 protein interactome.

Little is known about the CREB3 family interactome where only CREB3 has been most studied. A number of interacting partners have been identified for CREB3 including transcriptional coactivator HCF-1, hepatitius C virus core protein, CC chemokine receptor 1, dendritic cell specific transmembrane DC-Stamp, and ER lectin OS9 (21-24). Interestingly, data suggests that CREB3L1 does not function as a homodimer (25). Thus, this information suggests that if CREB3L1 forms dimers, these will be with other bZIP proteins. A further intriguing prospect is that CREB3L1 protein-to-protein interactions have cellular functions not limited to transcription. Indeed, full- CREB3L1 was recently shown to accumulate at the nuclear envelope in response to nuclear envelope stress supporting such a concept (26).

We have worked for several years on CREB3L1 in neuroendocrine cells of the rat supraoptic nucleus (SON) of the hypothalamus. We identified CREB3L1 expression in magnocellular vasopressin (AVP) and oxytocin (OXT) neurones, cells that synthesise and secrete vast quantities of neuropeptides releasing them centrally from axonal collaterals and peripherally from nerve terminals in the pituitary gland, and we have successfully characterised several functions in this brain nucleus in the regulation of hormone synthesis and secretion, ER stress, prohormone processing and more recently cellular proteostasis (13, 15, 27-30). One observation we have made in magnocellular neurones (MCNs) is vast quantities of CREB3L1 protein being seemingly sequestered in the cytoplasm in response to stimulation and we wanted to better understand its role in peptide hormone synthesis and secretion (12). This raises a pertinent question about CREB3L1 cellular functions, positioning us towards investigating the CREB3L1 interactome.

To identify protein interacting partners of CREB3L1 we created a prey library from the dehydrated SON, where peptide hormone synthesis and secretion is increased, and used an extend bZIP

domain as the bait for yeast two-hybrid screening. Our yeast two-hybrid approach identified five putative CREB3L1 interacting proteins, one of which was selected for detailed investigation. Thus, we identify cellular dimerisation hub protein Dynein Light Chain LC8-Type 1 (DYNLL1) as a CREB3L1 interacting protein and further show that this interaction enhances CREB3L1 activation of the *Avp* promoter.

2. Methods

2.1 Animals

All experiments were performed under Home Office UK licences 30/3278 and PP9294977 held under, and in strict accordance with, the provisions of the UK Animals (Scientific Procedures) Act (1986); they had also been approved by the University of Bristol Animal Welfare and Ethical Review Board. Animal sample sizes were calculated by making an estimate of variability from previous experiments that we have performed with two groups, using similar approaches, under similar conditions, in rats. These data provide an estimate of the expected standard deviation of the primary outcome and then power calculations were used to calculate the sample size for the experimental group (31). All studies were performed with time-matched experimental controls run in parallel and sampled on the same day. For animal studies with two groups, randomisation was performed by the flip of a coin to determine which group the animal was assigned.

Male Sprague Dawley rats weighing 250-274g were purchased from commercial supplier Envigo (RRID: 70508). Rats were housed under a 12:12 light/dark cycle at a temperature of 21-22°C and a relative humidity of 40-50% (v/v) with food and water *ad libitum* unless stated. Through the University of Bristol Animal Management Information System, animals are randomly assigned to cages by Animal Services Unit staff. The number of cages, and the number of animals per cage, is pre-set by the investigator on AMIS, but the allocation is independently performed. Rats were housed in groups of 3-4 for a 1–2-week period of acclimation before experimentation. Cages contained sawdust, bedding material, cardboard tubes, and wooden chews for enrichment. Water deprivation (WD) - For WD protocols drinking water was removed for 3 days beginning at the middle of the light phase. Salt loading (SL) - For the SL protocol drinking water was replaced with 2% (w/v) NaCl in drinking water for 7 days.

2.2 Yeast two-hybrid screening

A rat 3 days WD SON library (SONs pooled from 5 animals) was prepared starting from 2 µg of total RNA using Make Your Own “Mate & Plate” Library system in yeast strain Y187 (Clontech).

The library contained greater than 1 million independent clones with a titer of 1 x 10^8 cfu/ml. The Matchmaker Gold Yeast Two-Hybrid system (Clontech) was used to identify CREB3L1 interacting proteins. Rat CREB3L1 (amino acids 289-375) was used as bait by cloning in frame with the GAL4 DNA binding domain of the bait plasmid pGBKT7. The bait plasmid was transformed into yeast strain Y2H gold using Yeastmaker Yeast Transformation System 2 (Clontech) according to the manufacturer's protocol. Tryptophan positive clones were selected and concurrently assessed for autoactivation and toxicity. The yeast two-hybrid screen was performed as previously described (32). To recover the plasmids from positive clones, yeast cells were resuspended in 50 µl of lyticase in TE buffer (5 U/µl, Sigma-Aldrich, L4025) followed by vigorous vortexing. Then the mixtures were incubated at 37°C for 2 h with vortexing every 15 min. Next, glass beads and 10 µl of 20% (w/v) SDS were added into the mixtures followed by vigorous vortexing for 1 min. A Qiagen Plasmid miniprep extraction (Qiagen) was then performed according to the manufacturer's protocol. PCR amplification was performed on the recovered plasmids with screening primers (**Supplemental Table 1**) in the presence of 1 M betaine using Platinum Taq DNA polymerase (Thermo Fisher Scientific). The cycle conditions were 94 °C for 2 min, 35 cycles of 94°C for 30 sec, 60°C for 30 sec, 72°C for 3 min and a final extension at 72 °C for 5 min. The PCR products were electrophoretically separated on agarose gels to identify unique insert sizes. Plasmids were rescued by transformation to DH5α Competent Cells on ampicillin plates, followed by Qiagen plasmid miniprep extraction. cDNA harboring plasmids were sequenced by Eurofins Genomics Sequencing (Germany) and the cDNAs identified by nucleotide BLAST analysis.

2.3 Reverse transcription-quantitative polymerase chain reaction

The processing of brains for punching was randomised by using the balls in a bag principle to prevent processing bias. A 1 mm punch (Fine Scientific Tools, 18035-01) was used to collect SON and paraventricular nucleus (PVN) samples from coronal slices sectioned in a cryostat set at -20°C as previously reported (33). cDNA synthesis and qRT-PCRs were carried as described previously (30). For relative quantification of gene expression, the $2^{-\Delta\Delta CT}$ method was employed (34). The internal control gene used for these analyses was the housekeeping gene *Rpl19 (28, 29, 33)*. The qRT-PCR primer sequences can be found in **Supplemental Table 1**. Statistical analysis was performed on ΔCT values.

2.4 Immunofluorescence on brain slices

Perfusion fixation of tissue and slicing of brains was performed as described previously (33). Sections were washed 3x for 5 mins in phosphate buffered saline (PBS), then incubated in 10

mM sodium citrate buffer (pH6) at 95°C for 30 mins. Sections in sodium citrate buffer were placed at room temperature for 20 mins for cooling before being washed with PBS 3x, 5 mins each, then blocked and permeabilised in 3% (w/v) bovine serum albumen (BSA) prepared in 0.3% (v/v) triton-X100/PBS (PBS-T) for 30 mins at room temperature. Primary antibodies were prepared in 1% (w/v) BSA/PBS-T and incubated at 4°C for 24 h with constant rocking. After 3x 5 min washes in PBS, sections were incubated in darkness with secondary antibodies prepared in 1% (w/v) BSA/PBS-T for 1 h. Sections were washed 2x with PBS and incubated with DAPI (2-(4-amidinophenyl)-6-indolecarbamidinedihydrochloride, 1 µg/ml) prepared in PBS for 1 min. After washing with PBS, sections were mounted onto glass slides with 0.5% (w/v) gelatine (Sigma-Aldrich, G9382) and coverslipped with VectorShields hard set mounting media (Vector Laboratories). Confocal images were captured using an SP5-II confocal laser scanning microscope attached to a Leica DMI6000 inverted epifluorescence microscope (Leica Microsystems). Widefield images were captured using a Leica DMI6000 inverted epifluorescence microscope with Photometrics Prime 95 B sCMOS camera and Leica LAS-X acquisition software. The primary antibodies were goat polyclonal CREB3L1 antibody (1:1000, R and D Systems Cat# AF4080, RRID:AB_2086044), rabbit monoclonal DYNLL1/PIN antibody (1:500, Abcam Cat# ab51603, RRID:AB_2093654), mouse monoclonal anti-oxytocin-neurophysin antibody (1:200, clone PS 38 Cat# No. PS-38, RRID: AB_2315026 and mouse monoclonal anti-vasopressin-neurophysin antibody (1:200, clone PS 41 Cat# PS41, RRID: AB_2313960) both kindly gifted by Professor Harold Gainer. The secondary antibodies donkey anti-goat Alexa 594 (1:500; Thermo Fisher Scientific Cat# A-11058 (also A11058), RRID:AB_2534105) and donkey anti-rabbit Alexa 488 (dilution 1:500; Thermo Fisher Scientific Cat# A-21203, RRID:AB_141633).

2.5 Cell culture

Mouse pituitary cell line AtT20/D16v-F2 (ECACC Cat# 94050406, RRID:CVCL_4109) (AtT20) and Human Embryonic Kidney cells HEK293T/17 (ATCC, CRL-11268, RRID:CVCL_1926) (HEK) were cultured in DMEM (Sigma, D6546) supplemented with 10% (v/v) heat-inactivated foetal bovine serum (Sigma-Aldrich; F9665), 2 mM L-glutamine (Gibco, 25030) and 100 unit/ml of penicillin-streptomycin (Gibco, 15140). Cells were incubated at 37°C in a humidified incubator with 5% (v/v) CO_2. Cells were seeded onto tissue culture plates to 60%–70% confluence for experiments. Chemical treatments were performed at the time points indicated in the figure; vehicle DMSO or 10 µM forskolin (FSK; Sigma). Stock solutions of FSK were prepared to 10 mM with DMSO.

2.6 Creb3l1 mutants

Mutants, mTQT, of rat *Creb3l1* were generated by overlap extension PCR using Phusion High-Fidelity DNA Polymerase (New England BioLabs). The amino acid sequence of the putative DYNLL1 interaction site was mutated from MA**ATQ**TGT to MA**TAG**TGT by converting the glutamine at position 0 to a glycine and switching the position of amino acids at positions -1 and -2. See **Supplemental Table 1** for primer details.

2.7 Dynll1 cell lines

To produce knockdown cell lines, cells were transduced with a lentivirus containing an shRNA targeting human *Dynll1* as previously described (35). Sense and antisense oligonucleotides (Supplemental Table 1) for this shRNA were annealed and ligated into lentiviral transfer vector pLKO.1 puro according to manufacturer's guidelines (pLKO.1 puro was a gift from Bob Weinberg, Addgene plasmid 8453). The non-targeting (NT) shRNA sequence used as a control has previously been described (35). Virus particles were produced in HEK cells as previously described (12). Twenty-four hours after transduction, culture media was replaced with fresh media containing puromycin (2 µg/ml, Thermo Fisher Scientific). Transduced cells were cultured in the presence of puromycin for 2 weeks before use in experiments where puromycin was removed. The polygenic HA tag Dynll1 overexpressing AtT20 cell line was prepared by selection with 500 µg/ml G418 for 4 weeks.

2.8 Immunofluorescence of cells

Cells were grown on coverslips in 12-well tissue culture plates to reach 60%–70% confluence the day after seeding. Transfections were performed the day after using Lipofectamine LTX transfection reagent (Thermo Fisher Scientific). At 48 h after transfections cells were fixed with 4% (w⁄v) paraformaldehyde (PFA) in PBS for 10 min followed by 3x washes with PBS for 5 mins each. Cells were then incubated with 0.3% (v⁄v) Triton X-100 in PBS for 10 min for permeabilisation followed by 5% (v/v) horse serum prepared in PBS with 0.03% (v⁄v) Triton X-100 (PBS3T) for 30 min for blocking. Cells were incubated in primary antibody prepared in 1% (v⁄v) horse serum in PBS3T at 4°C overnight. After 3x washes, cells were incubated in secondary antibody prepared in 1% (v⁄v) horse serum in PBS3T for 1 h at room temperature. Coverslips were mounted onto glass slides using VectorShields hard mounting media with DAPI. Confocal images were captured using an SP5-II confocal laser scanning microscope attached to a Leica DMI6000 inverted epifluorescence microscope (Leica Microsystems). Primary antibodies were anti-HA tag antibody (1:2500, Abcam Cat# ab9110, RRID:AB_307019), Monoclonal ANTI-FLAG®

M2 antibody produced in mouse (1:1000, Sigma-Aldrich Cat# F1804, RRID:AB_262044) and goat polyclonal CREB3L1 antibody (1:2000, R and D Systems Cat# AF4080, RRID:AB_2086044). Secondary antibodies donkey anti-mouse Alexa 594 (dilution 1:500; (Thermo Fisher Scientific Cat# A-21203, RRID:AB 141633), donkey anti-rabbit Alexa 488 (1:500), and donkey anti-goat Alexa 594.

2.9 Western blotting

Cells were seeded into 3 cm dishes (1 x 10^6 cells). Transfections with *Creb3l1* constructs (2.5 µg) were performed the next day using Lipofectamine® 3000 (Thermo Fisher Scientific) following the manufacturers guidelines. After 48 h, cells were washed with PBS and harvested by scraping in 500 µl of radioimmunoprecipitation assay (RIPA, 25 mM Tris-HCl, pH 7.6; 150 mM NaCl; 1% (v/v) Nonidet P-40; 1% (v/v) sodium deoxycholate; 0.1% (w/v) sodium dodecyl sulfate; 1 mM EDTA) buffer supplemented with protease inhibitor cocktail (Sigma-Aldrich, P8340). Lysate was incubated on ice for 15 min with vortexing every 5 min. Debris was removed by centrifugation at 10,000 ×g for 10 min. Protein concentrations were determined by the Bradford assay performed with BSA standards.

Protein samples were subjected to sodium dodecyl sulphate-polyacrylamide gel electrophoresis, then transferred to 0.45 µm polyvinylidene fluoride membrane (MERCK). Membranes were blocked for 1 h using 1% (w/v) ECL Advance Blocking Reagent (Sigma-Aldrich) prepared in Tris buffered saline (TBS) + 0.1% (v/v) Tween 20 (blocking solution). Next, primary antibodies were diluted in blocking solution and incubated at 4˚C overnight with gentle rocking. Membranes were washed 3x for 5 min each in TBS-T and then incubated for 1 h with Clean-Blot IP Detection Reagent (HRP) (Thermo Fisher Scientific Cat# 21230, RRID:AB_2864363) diluted in blocking solution. Membranes were washed 3x for 5 min each in TBS-T. The signal was visualized by chemiluminescence using Supersignal West Dura chemiluminescent substrate (Thermo Fisher Scientific). Images were captured using a Syngene G:Box XT4 (Syngene, Cambridge, UK). Primary antibodies used were a goat CREB3L1 antibody (1:1000, R and D Systems Cat# AF4080, RRID:AB_2086044) and anti-HA tag antibody (1:2500, Cell Signaling Technology Cat# 2367, RRID:AB_10691311).

2.10 Co-immunoprecipitation

To investigate if CREB3L1 and DYNLL1 interact in mammalian cells, HEK cells (1 × 10^7 cells) were seeded onto 15 cm tissue culture plates and co-transfected with 3xHA tagged rat *Dynll1*

plasmid construct (10 µg) and FLAG tagged rat *Creb3l1* plasmid constructs (each 10 µg). Transfections were performed the day after seeding using Lipofectamine® 3000 following the manufacturer's guidelines (Thermo Fisher Scientific). 48 h after transfection, cells were washed 2x in PBS before being lysed in lysis buffer (50 mM Tris HCl, pH 7.4, with 150 mM NaCl, 1 mM EDTA, and 1% Triton X-100) supplemented with protease inhibitor cocktail (Sigma-Aldrich, P8340). Lysates were transferred to 1.5 ml tubes and incubated on ice for 15 mins (with regular mixing by pipetting at 5 min intervals). Lysates were centrifuged at 10,000 ×g at 4ºC for 15 mins. Protein concentrations were determined by the Bradford assay and 500 µg of total protein was prepared to a volume of 1 ml with lysis buffer. To pull-down CREB3L1, 50 µl anti-FLAG-M2 magnetic beads (Sigma-Aldrich Cat# M8823 (also M8823-1ML, M8823-5ML), RRID:AB_2637089) and for DYNLL1 pull-downs 2 µg of anti-HA tag antibody (Abcam Cat# ab9110, RRID:AB_307019) was added to protein samples in lysis buffer. Samples were placed at 4ºC overnight on a tube rotator (VWR). Flag constructs – tubes were placed in a magnetic separator to collect the beads and the supernatant was discarded. The magnetic beads were washed 5x with 1 ml of TBS (50 mM Tris HCl, pH 7.4, with 150 mM NaCl). HA construct – 25 µl of Dynabeads® Protein G magnetic beads (Thermo Fisher Scientific) were added to each sample. The samples were placed at 4ºC for 1 h on a tube rotator (VWR) and then washed 5x as described above. Protein complexes were eluted from magnetic beads by boiling for 3 mins in SDS page sample buffer made up of 2% (w/v) sodium dodecyl sulfate , 10% (v/v) glycerol, 5% (v/v) 2-mercaptoethanol, 0.002% (w/v) bromophenol blue and 0.125 M Tris HCl, pH 6.8).

2.11 Proximity ligation assay

To visualize the protein proximity of CREB3L1 and DYNLL1 in the cell Duolink proximity ligation assays (Sigma-Aldrich) were performed in HEK and AtT20 cells. Cells seeded onto coverslips were fixed with 4% PFA and washed and permebilised as described for immunostaining. Coverslips were removed from the plate and placed cell side down onto 40 µl droplets of Duolink Blocking solution on parafilm in a humidified chamber which was placed into a 37°C incubator for 30 mins. Primary antibodies were diluted at the dilutions used described for immunostaining in Duolink Antibody Diluent. The blocking solution was wicked off the coverslips by gently tapping the corner onto mediwipes and coverslips were placed onto 40 µl droplets of primary antibody solution and incubated in a humidified chamber at 4°C overnight. Coverslips were placed back into 12-well tissue culture plates and washed 2x for 5 min each in 1 ml wash buffer A. Next, coverslips were placed onto droplets of 40 µl Duolink PLA probe solution and incubated in a humidity chamber for 1 h at 37°C. Coverslips were placed back into 12-well tissue culture plates

and washed 2x for 5 min each in 1 ml wash buffer A. Next, coverslips were placed onto droplets of 40 µl Duolink PLA ligation solution and incubated in a humidity chamber for 30 mins at 37°C. After a further 2x washes in wash buffer A, coverlips were placed onto droplets of 40 µl Duolink PLA amplification solution and incubated in a humidity chamber for 100 mins at 37°C. Coverslips were washed for 2x 10 mins in 1x wash buffer followed by a 1 min wash in 0.01x wash buffer B. Coverslips were mounted on slides using Duolink *in situ* mounting media with DAPI.

2.12 Luciferase assays

The *Col1a1* promoter was amplified from rat liver genomic DNA with primers possessing restriction sites for digestion and annealing and cloning into compatible sites of pGL4.10[*luc2*] basic Vector (Promega, E6651). Primers details are found in **Supplemental Table 1**. The cloning of the *Avp* promoter has previously been described (12). Luciferase assays were performed as described previously using Dual Luciferase Reporter Assay System (Promega, E1910) (15). To transfect DNA into cells Lipofectamine LTX (Thermo Fisher Scientific) was used on cells seeded in 12-well plates. For Dynll1 knockdown cell studies, 0.1 µg of pGL4-Avp promoter was co-transfected with 0.9 µg of pcDNA empty plasmid or *Creb3l1* construct. For *Dynll1* overexpression studies, 0.1 µg of pGL4-promoter construct (*Avp* or *Col1a1*) was co-transfected with 0.4 µg of pcDNA and/or Creb3l1 and/or Dynll1. Each transfected well contained 2 ng control renilla reporter pRL-CMV (Promega, E2261). Samples were collected 24 h post transfection.

2.13 Statistical analysis

Image brightness and contrast adjustments were made to the whole image in Leica LAS X software. Statistical analyses and plotting of data were performed in GraphPad Prism version 9. Statistical differences between two experimental groups were evaluated using independent-sample unpaired t tests. One-way ANOVA with Dunnett's *post hoc* tests were used to determine the difference between more than two samples with only a single influencing factor. Two-way ANOVA with a Šídák method *post hoc* test was used for luciferase assay data. The data are presented as the mean ± SEM where $p \leq 0.05$ was considered statistically significant.

3. Results

3.1 Identification of putative CREB3L1 interacting proteins by yeast two-hybrid screening

We performed a yeast two-hybrid screen to identify CREB3L1 interacting proteins in the SON. Our experimental protocol is detailed in **Fig. 1A**. The yeast two-hybrid screen identified 5 potential CREB3L1 interacting proteins which were DYNLL1, Dynein Light Chain LC8-Type 2 (DYNLL2),

Axin Interactor, Dorsalization Associated (AIDA), OS9, and Heat Shock Protein Family A (Hsp70) Member 14 (HSPA14) (**Fig. 1B**). Notably, most screened clones corresponded to DYNLL1. The DYNLL proteins are homodimer proteins that were first shown to interact with dynein and myosin 5a motor proteins but are now known to interact with many proteins and are recognized as regulator hub proteins for diverse cellular functions. OS9 is a lectin which functions in quality control in the endoplasmic reticulum and ER-associated degradation. HSPA14 belongs to the heat shock protein family A (HSP70) and is involved in cellular processes such as protein folding, preventing protein aggregation, and protein degradation. AIDA is an AXIN, a cell scaffold protein, interacting protein that negatively regulates the Axin-mediate JNK pathway by disrupting Axin homodimerisation.

To select candidate/s for further investigation we inputted our identified proteins into the STRING database to obtain information about currently known protein-to-protein associations. The string resource revealed no known interactions between CREB3L1 and these 5 proteins, so we have included dashed lines to represent out putative interactions from yeast two-hybrid (**Fig. 1C**). However, known interactions were displayed between the two DYNNL proteins. We next asked about known protein-to-protein associations with the CREB3 family (**Fig. 1D**). This showed OS9 as an experimentally validated CREB3 interacting protein. To discover novel functional interactions for the CREB3 family we decided to focus on the DYNLL proteins the most numerous identified interactors from our yeast two-hybrid screen.

The DYNLL proteins bind to short linear motifs in intrinsically disordered protein segments. This interaction is often mediated by TQT motifs. In our bait sequence we identified a single TQT motif C-terminal to the bZIP domain at amino acids 369-371 (T369 Q370 T371) that was conserved in human and mouse (**Fig. 1E**). Notably, the entire CREB3L1 protein possesses only a single TQT motif. We next asked if TQT motifs featured in other members of the CREB3 family. Sequence mining showed that only CREB3L2 contains a TQT domain interestingly in the same location as for CREB3L1 (**Fig. 1F**). Sequence alignments were performed using Clustal Omega (36). To investigate the presence of DYNLL binding domains, as non-canonical interaction domains have also been identified for some proteins, we searched the Harmonizome 3.0 database for DYNLL potential interactors from the curated Hub Proteins Protein-to-Protein Interactions dataset (37). This revealed only CREB3L2 as a potential DYNLL interactor consistent with our observation of a TQT motif.

3.2 Osmotic stimulation of the supraoptic nucleus increases *Dynll1* expression

We next investigated SON *Dynll1* and *Dynll2* expression in different physiological conditions that increase CREB3L1 expression and increase AVP and OXT synthesis and release (**Fig. 2**). We have previously published data from these animals for AVP and OXT synthesis and secretion (38). There were significant (on-way ANOVA) alterations to *Dynll1* expression in the SON following chronic osmotic challenge ($F_{2,15} = 8.813$, $p = 0.0029$). Dunnet's multiple comparisons test showed that WD and SL significantly increased *Dynll1* expression (3 d WD, $p = 0.002$; 7 d SL, $p = 0.017$) (**Fig. 2A**). We found no difference in *Dynll2* expression in the SONs of 3 d WD and 7 d SL rats (**Fig. 2A**). We next looked at DYNLL1 protein expression in the SON of control and 3 d WD rats by immunofluorescence (**Fig. 2B**). The expression of DYNLL11 was observed in MCNs in the SON. As expected, CREB3L1 expression was dramatically increased by WD whereas DYNLL1 expression and cellular distribution appeared unaltered by WD. Higher magnification confocal microscope images showed that DYNLL1 is expressed in both the cytosolic and nuclear cellular compartments of MCNs (**Fig. 2C**). Confocal images in control rats showed CREB3L1 staining in perinuclear areas of MCNs, whereas following WD, staining was observed throughout the cell cytoplasm. This striking increase in CREB3L1 in the cytosolic compartment of WD MCNs, as we have previously reported (12), resulted in increased co-expression with DYNLL1 in this cellular compartment.

3.3 Confirmation of CREB3L1-DYNLL1 interactions via a single TQT motif

To investigate interactions between CREB3L1 and DYNLL1 in mammalian cells we created a series of N-terminal FLAG tagged CREB3L1 mutants to test in HEK cells (**Fig 3A**). In transfections with a CREB3L1FL TQT (FL-mTQT) mutant we show that cleavage of CREB3L1 is not altered (**Fig. 3B**). The expected full-length immunoreactive form of CREB3L1 with a molecular weight close to 80 kDa was present in the FL-TQT mutant and control FL transfected cells. Furthermore, the immunoreactive CREB3L1 doublet migrating close to 60 kDa, formed by the cleavage steps of S1P and S2P during RIP, was present in similar ratios in FL-TQT and control FL transfected cells.

We next investigated the cellular localisation of CREB3L1 and DYNLL1 in HEK cells (**Fig. 3C**). As previously reported, CREB3L1 was expressed predominantly in the cell cytoplasm. In contrast, DYNLL1 expression exhibited a more even distribution throughout cellular compartments, though still predominantly in the cytoplasm, as previously described (39-42). Thus, co-expression of CREB3L1 and DYNLL1 was observed in the cytoplasm. The FL-mTQT did not alter the

distribution of CREB3L1 or DYNLL1 immunofluorescent staining compared to control FL transfected cells. We next looked at the expression of CA CREB3L1 (**Fig. 3D**). Here, staining was predominantly located in the nucleus consistent with previous observations in several cell-types (5, 13, 43). Interestingly, cells with abundant CA in the nucleus also had increased nuclear DYNLL1 expression compared to both FL transfections. Thus, in this case, co-expression of CREB3L1 and DYNLL1 occurred in the nucleus. We created an additional TQT mutant for constitutively active CREB3L1 (CA), CA-mTQT, to establish if the TQT domain was important for nuclear translocation (**Fig. 3B**). The expression of CA-mTQT still strongly localised to the nucleus. However, unlike CA, DYNLL1 expression was not increased in the nucleus, exhibiting a similar distribution to both FL transfections suggesting that association with CREB3L1 promotes DYNLL1 nuclear translocation.

To confirm the CREB3L1-DYNLL1 protein-to-protein interaction in HEK cells we performed a series of co-immunoprecipitations with tagged *Creb3l1* and *Dynll1* constructs (**Fig. 3E**). All CREBL1 forms were captured by FLAG tagged magnetic beads and the success of immunoprecipitations confirmed by probing immunopreciptates with a FLAG antibody. Both FL and cleaved forms of CREB3L1 were present in immunoprecipitations from FL and FL-TQT transfections. However, DYNLL1 expression was exclusively found in immunoprecipitates derived from FL but not FL-mTQT. In support of this domain being the major site of interaction, DYNLL1 was present only in immunopreciptates from CA and not CA-TQT. Moreover, the capture of DYNLL1 appeared greater in CA suggesting that CREB3L1-DYNNL1 interactions occur post RIP.

3.4 Stimulation of CREB3L1 expression by cAMP pathways leads to increased interactions with DYNLL1

To further investigate CREB3L1-DYNLL1 interactions in different cellular compartments we performed proximity ligation assays (PLA) in HEK cells (**Fig. 4A**). All controls showed no specific signal. However, immunofluorescent puncta were observed in the PLA protocol (**Fig. 4B**). Immunofluorescent puncta were present in the cytoplasm and nucleus of HEK cells suggesting interactions in both cellular compartments. We next asked if stimuli that increase endogenous CREB3L1 expression and activation by cleavage alters interactions. We used our model of activation by cAMP pathways in mouse pituitary cell line AtT20. As the DYNLL1 antibody did not work for PLA, we generated a stable polygenic HA tag *Dynll1* overexpressing AtT20 cell line with an empty pcDNA control cell line. The expression of DYNLL1 was observed in the cytoplasm and nucleus of AtT20 cells by immunofluorescence and stimulation by FSK significantly increased

CREB3L1 expression (**Fig. 4C**). We next performed immunoprecipitations of DYNLL1 in AtT20 cells treated with vehicle or FSK (**Fig. 4D**). Interestingly, a distinct CREB3L1 immunoreactive band corresponding to the molecular weight of cleaved CREB3L1 was observed in immunoprecipitates from FSK treated *Dynll1* AtT20 cells. Thus, we proposed that the stimulation of CREB3L1 expression increases interactions with DYNLL1 in AtT20 cells. We tested this hypothesis by PLA in *Dynll1* AtT20 cells treated with vehicle or FSK (**Fig. 4E**). Controls showed a low level of background signal. The PLA showed fluorescent puncta in both the cytoplasm and nucleus of AtT20 cells. Combined, these data suggest that stimulation of CREB3L1 expression by cAMP pathways promotes increased interaction with DYNLL1.

3.5 DYNLL1 is a positive regulator of CREB3L1 transcriptional activity

To functionally investigate the CREB3L1-DYNLL1 interaction we performed promoter luciferase reporter assays in HEK cells (**Fig. 5A**). We firstly generated a stable polygenic HEK *Dynll1* knockdown and a scrambled control cell line. These knockdown cells exhibited >50% knockdown compared to the scrambled control ($t = 11.91$, $p < 0.001$) (**Fig. 5B**). We next asked if the transcriptional output of FL and CA was altered by the depletion of *Dynll1* expression using our well-established target, the rat *Avp* promoter. A two-way ANOVA revealed that knockdown significantly altered transactivation of the *Avp* promoter ($F_{1,12} = 196.7$, $p < 0.001$). Sidak's multiple comparisons test found that knockdown significantly reduced promoter activity in cells transfected with FL ($p = 0.005$), and CA ($p < 0.001$) (**Fig. 5C**). That HEK cells endogenously express *Creb3l1* possibly accounts for diminished luciferase activity in control samples. These data suggested DYNLL1 binds to and positively regulates CREB3L1 transcriptional activity.

To further challenge this hypothesis, we performed luciferase reporter assays following overexpression of *Dynll1* in HEK cells transfected with different *Creb3l1* constructs (**Fig. 5D**). A two-way ANOVA revealed that *Dynll1* overexpression significantly altered transactivation of the *Avp* promoter by CREB3L1 ($F_{1,20} = 82.87$, $p < 0.001$). The combined overexpression of FL and Dynll1 significantly increased ($p = 0.04$) luciferase activity whereas FL-TQT had no effect. Furthermore, the overexpression of CA and *Dynll1* significantly increased (by 36%, $p < 0.001$) luciferase activity whereas CA-TQT and *Dynll1* did not as determined by Sidak's post hoc test. We next asked if CREB3L1 activation of the mouse *Col1a1* promoter, another well-established target (6), was altered (**Fig. 5E**). A two-way ANOVA revealed that *Dynll1* overexpression significantly alters *Col1a1* promoter activation mediated by CREB3L1 ($F_{1,20} = 221$, $p < 0.001$). We identified increased promoter activity for both FL ($p < 0.001$) and FL-TQT ($p < 0.001$) in the

presence of *Dynll1* compared to controls transfected cells as determined by Sidak's post hoc test. The overexpression of CA and *Dynll1* significantly increased (by 37%, $p < 0.001$) luciferase activity while CA-TQT and *Dynll1* did not as determined by Sidak's post hoc test. Therefore, interactions between CREB3L1 and DYNLL1 can significantly enhance transcriptional activity.

4. Discussion

Transcription factors can potentially complex with multiple proteins in the process of transcriptional regulation. It is the investigation of these interactomes that provides a greater understanding of DNA binding protein functions and regulation. Here, we performed a yeast two-hybrid screen using a bespoke SON prey library to investigate the CREB3L1 protein-to-protein interactome. This screen identified five candidate CREB3L1 interacting proteins for further study. To choose our candidate protein we integrated information from available protein-to-protein interaction databases to guide our selection process. Here we have identified for the first time CREB3L1 as a DYNLL1 interacting protein and show this interaction can enhance CREB3L1 transcriptional output.

DYNLL1 has been described as a hub protein and dimerisation engine that is involved in many interactions that are central to cellular functions. DYNLL1 was first called PIN, **P**rotein **I**nhibitor of **N**itric oxide synthase (NOS), after being identified as a NOS interactor from a hippocampal yeast two-hybrid library screen, and subsequently shown to inhibit NOS dimerisation (44). A later study in neurons suggested that IFN-γ upregulates NOS-1 by initiating the proteasomal degradation of DYNLL1 leading to increased NOS dimerisation (45). Thus, DYNLL1, by interacting with NOS-1 can influence neuronal signalling molecules. Moreover, in insulin-secreting beta-cells, DYNLL1 associates with insulin secretory granules where it colocalises with NOS1 (40). The overexpression of *Dynll1* in cell line Ins-1 results in enhanced glucose stimulated insulin secretion suggesting an important functional role in endocrine cells. In the brain NOS-1 can exist as a ternary complex with carboxy-terminal PDZ ligand CAPON and RASD1 (dexamethasone inducible Ras protein 1) (46). MCNs neurones of the SON express NOS1, CAPON, and RASD1 and water deprivation increases *Nos1*, *Dynll1*, *Rasd1* and *Creb3l1* expression but any interplay between proteins and complexes remains to be explored (47).

What have shown that a TQT binding motif facilitates the CREB3L1-DYNLL1 interaction. The TQT motif GLN (Q) at position 0 is crucial for DYNLL1 protein interactions, with hydrophobic residues (T) at -1 and +1 also being important (48). Indeed, sited-directed mutation of this motif prevents

CREB3L1-DYNLL1 interaction. The close proximity of TQT motifs to coiled coil and dimerisation domains is a feature of DYNLL1-binding proteins (48). It has been proposed that DYNLL1 functions like a molecular glue to stabilise dimeric structures with many DYNLL1 binding partners known to exist as homodimers (48). The bZIP transcription factors function a homo and/or heterodimers to regulate both binding site specificity and transcriptional activity. Heterodimers of CREB3L1-CREB3L4 and CREB3L1-CREB3 have been proposed during investigation of promoter luciferase activity in neural precursor cells (19). Therefore, one possibility is that DYNLL functions as a molecular glue for CREB3L1 heterodimerisation, with one candidate protein identified here being CREB3L2.

Interactions between DYNLL1 and several other transcription factors have been described. A yeast two-hybrid screen identified Nuclear respiratory factor 1-DYNLL1 interactions and *in vitro* studies described co-localisation of these proteins in the nucleus of C6 glioma and Balb/3T3 cells (49). ASCIZ, which is a transcriptional factor of the *Dynll1* gene, contains several TQT motifs and DYNLL1 interactions alter its transcriptional activity (41). In addition, TRPS1-DYNLL1 interactions have been described in the nucleus of primary human fibroblasts, and by using a GATA luciferase reporter, DYNLL1 was shown to suppress the transcriptional repression activity of this transcription factor in HepG2 cells (39). In breast cancer cells estrogen receptor-DYNLL1 interactions enhance the recruitment of the estrogen receptor to target gene chromatin (42). Subsequently, knocking down *Dynll1 expression* decreases estrogen receptor-transactivation activity and estrogen receptor nuclear accumulation, suggesting that DYNLL1 is a chaperone for cytosolic to nuclear translocation of this receptor. In contrast, our data suggests that CREB3L1 chaperones DYNLL1 to the nucleus. It is predicted that CREB3L1 contains a single bipartite nuclear localization signal that is highly conserved across vertebrates, which would appear sufficient for CREB3L1 nuclear translocation. A single amino acid deletion in the predicted nuclear localization signal was identified as the cause of Osteogenesis Imperfecta in a human study (25). Interestingly, DYNLL1 overexpressing transgenic mice exhibit a mild osteopetrotic phenotype with increased bone mineral density (50) with the opposite phenotype of that observed in CREB3L1 knockout mice (6). Thus, it will be of interest to investigate how the CREB3L1-DYNLL1 interaction modifies the CREB3L1 target transcriptome in secretory cell-types.

In astrocytes, CREB3L1 is cleaved in response to DNA damage where it then acts on target genes including p21 to induce cell cycle arrest independently of cell cycle regulator p53 (18). Interestingly, DYNLL1 interacts with p53 binding protein, p53BP1, a key mediator in the repair of

double-strand breaks serving as a scaffold at damaged chromatin to uphold genomic stability (51). Furthermore, DYNLL1 interacts with p21 activated kinase PAK1, which also has roles in the cell cycle, and the PAK1-DYNLL1 complex has been shown to be necessary for epidermal growth factor induced nuclear import of PAK1 in MCF-7 cells (52). Moreover, DYNNL1 has been alluded to as a universal regulator of DNA repair through its interactions with numerous proteins (53). Thus, the CREB3L1-DYNLL1 complex may represent part of the DYNLL1 chain in cell cycle control. This could be as a transcription factor or possibly via non-transcriptional actions as recently highlighted by CREB3L1 functions in nuclear envelope stress (26).

Whilst one of five possible interactors identified in this study was investigated further, we here briefly discuss the other four possible interactors in relation to biological processes mediated by CREB3L1. 1. OS9 has previously been identified as a CREB3 interacting protein and is upregulated in response to ER stress where it associates with components of the ER-associated protein degradation (ERAD) machinery as well as with ER substrates to facilitate the ubiquitination of misfolded glycoproteins (21, 54). It was proposed in that CREB3-OS9 interaction regulates the stability and turnover of CREB3. 2. HSPA14 forms a heterodimer with DnaJ Heat Shock Protein Family (Hsp40) Member C2 that forms the ribosome-associated complex, a chaperone that spans ribosomes at positions that can sense and co-ordinate translation and protein folding (55). Interestingly, inhibiting the ribosome-associated complex leads to the reduced activation of ER transmembrane sensor IRE1 of the unfolded protein response by preventing IRE1 oligomerisation in response to ER stress with reduced production of spliced X-box binding protein 1 (*Xbp1*) (56). It is known that CREB3L1 is a transcription factor for *Xbp1* and *Bip* with the later known to be a binding protein of IRE1 (4, 57). Thus, the potential CREB3L1-HSPA14 represents an exciting and additional path to explore CREB3L1 in ER stress and proteostasis. 3. In mice, AIDA was identified as a component of ERAD that selectively controls ERAD-mediated degradation of triacylglycerol synthesis enzymes (58). 4. DYNLL2 expression increases in PVN OXT neurones of fed compared to fasted rats and we have shown that OXT neurones express CREB3L1 (59). Thus, we have identified four additional potential CREB3L1 interactors that represent interesting targets for further investigation.

4.1 Limitations

The collection of the SON enriches for MCNs, so we acknowledge that the yeast prey library has been made from RNAs derived from the SON region which includes other cell-types such as glia. To investigate cell-type specific CREB3L1-DYNLL1 interactions, we performed PLA on brain

slices, but this technique was not successful on tissue. Therefore, we were not able to confirm if this protein interaction occurs in MCNs or glial cells in the SON, which both express CREB3L1. However, the significant enhancement in *Avp* promoter activity resulting from *Dynll1* overexpression suggests an important role for this novel interaction in peptide hormone synthesis by MCNs, and likely other endocrine systems. Increased *Avp* transcription could result in increased peptide biosynthesis and secretion by MCNs although this remains to be established. Notably, we also performed a yeast two-hybrid screen with full-length rat CREB3L1 protein but did identify any interacting proteins. Thus, our study describes protein interactions with only a portion of the CREB3L1 protein.

5. Conclusion

In summary, we identify a DYNLL1-CREB3L1 protein-to-protein interaction that enhances transcriptional activation of CREB3L1 target genes. In WD SONs where *Creb3l1* and *Dynll1* expression increases, this mechanism could help to shape the CREB3L1 target transcriptome to support increased demands for the synthesis of peptides including AVP and OXT. As AVP and OXT are also synthesised by MCNs and parvocellular neurones in the PVN and AVP neurones in the suprachiasmatic nucleus which express CREB3L1, the DYNLL1-CREB3L1 protein-to-protein interaction could be crucial for the elaboration of these peptides and other peptides. The broad interest in these findings lies in the investigation of CREB3L1-DYNLL1 interactions, as well as other possible interacting proteins identified in this study, in CREB3L1 expressing systems in health and disease.

6. Acknowledgements

We would like to thank the Wolfson Bioimaging Facility. Diagrams were created with BioRender.com. This research was supported by the Medical Research Council (Grants MR/W028999/1 and MR/N022807/1) to MPG, MG, and DM and Biotechnology and Biological Sciences Research Council (BB/R016879/1) to MPG and DM. BTG was supported by the Biotechnology and Biological Sciences Research Council-SWBio DTP programme (BBSRC BB/M009122/1). Diagrams were created with BioRender.com.

7. Author contributions

Mingkwan Greenwood: Conceptualization, Data curation, Investigation, Methodology, Supervision, Validation, Visualization, and Writing - review & editing. **Benjamin Gillard:** Data

curation, Investigation, Methodology, and Writing - review & editing. **David Murphy:** Conceptualization, Funding acquisition, Project administration, and Writing - review & editing. **Michael Paul Greenwood:** Conceptualization, Data curation, Formal analysis, Funding acquisition, Investigation, Methodology, Project administration, Supervision, Validation, Visualization, and Writing original draft.

8. Data availability

All novel materials and raw data are available to the community upon request to the corresponding author.

9. Figure legends

Figure 1. Identification of putative CREB3L1 interacting proteins by yeast two-hybrid screening. A, experimental protocol for CREB3L1 yeast two-hybrid screening. B, CREB3L1 interacting proteins identified in the prey library. C, investigation of the connectivity of possible CREB3L1 interactors by STRING. D, investigation of the connectivity of possible CREB3L1 interactors including all CREB3 family members by STRING. E, sequence alignment of potential DYNLL interacting motif for selected mammalian CREB3L1 sequences. F, sequence alignment of rat CREB3L1 and CREB3L2 TQT motifs. Lines connecting nodes: turquoise, known interaction from curated database; purple, known interaction experimentally determined; dark blue, predicted interaction gene occurrence; yellow, text mining; black, co-expression; light blue, protein homology; dashed line, putative interaction identified here by yeast two-hybrid.

Figure 2. Osmotic stimulation of the supraoptic nucleus increases *Dynll1* expression. A, relative mRNA expression of *Dynll1 and Dynll2* was investigated by qRT-PCR in the SON and PVN of 3 day WD and 7 day salt loaded (SL) male rats. B, immunostaining of CREB3L1, DYNLL1, AVP and OXT in control and 3-day WD rats. C, higher magnification confocal images of CREB3L1 and DYNLL1 staining in MCNs of control and 3-day WD rats. Scale bars = 100 μm (B), 25 μm (C) and 10 μm (zoom). WD, water deprived; SL, salt loaded. Values are means + SEM of n = 3 per group. $*p \leq 0.05$ and $**p \leq 0.01$.

Figure 3. Confirmation of DYNLL1-CREB3L1 interactions via a TQT motif. A, diagram of site directed mutations of FL and cleaved CA CREB3L1. B, immunoblot of CREB3L1 in HEK cells transfected with FL, FL-mTQT, CA and CA-mTQT constructs. C, CREB3L1 and DYNLL1 immunofluorescence in HEK cells transfected with plasmid-expressing FL or FL-mTQT and

Dynll1. D, CREB3L1 and DYNLL1 immunofluorescence in HEK cells transfected with plasmid-expressing CA or CA-mTQT and *Dynll1*. E, immunoblots of CREB3L1 and DYNLL1 expression in input samples and FLAG-CREB3L1 immunoprecipitates from HEK cells transfected with constructs FL or FL-mTQT or CA or CA-mTQT and *Dynll1*. Scale bars = 25 μm.

Figure 4. Stimulation of CREB3L1 by cAMP pathways leads to increased interactions with DYNLL1. A, diagram of the PLA experimental protocol. B, PLA assay in HEK cells transfected with constructs FL and *Dynll1*. Antibody controls were performed with no antibody, HA antibody only or FLAG antibody only. PLA includes both HA and FLAG antibodies. C, immunofluorescence of DYNLL1 and CREB3L1 in stable *Dynll1* AtT20 cells treated with vehicle or forskolin (FSK) for 6 hours. D, immunoblot of CREB3L1 expression in input (In) samples and HA-Dynll1 immunoprecipitates (IP) from pcDNA and *Dynll1* AtT20 cells treated with vehicle or FSK for 6 hours. E, PLA assay in *Dynll1* AtT20 cells treated with vehicle of FSK for 6 hours. Antibody controls were performed with HA and CREB3L1 antibodies separately (ab cons). PLA includes both HA and CREB3L1 antibodies. Scale bars = 50 μm (B) and 25 μm (C and E). PLA, proximity ligation assay.

Figure 5. DYNLL1 is a positive regulator of CREB3L1 transcriptional activity. A, diagram of luciferase constructs. B, qRT-PCR assessment of shRNA mediated knockdown of *Dynll1* in HEK cells. C, *Avp* promoter luciferase assays in control and *Dynll1* knockdown HEK cells transfected with pcDNA, FL, or CA constructs. D, *Avp* promoter luciferase assays for the overexpression of *Dynll1* in combination with pcDNA, FL, FL-mTQT, CA, or CA-mTQT constructs. E, *Col1a1* promoter luciferase assays for overexpression of *Dynll1* in combination with pcDNA, FL, FL-mTQT, CA, or CA-mTQT constructs. Values are means + SEM of n = 3 per group. $*p \leq 0.05$, $**p \leq 0.01$, $***p \leq 0.001$.

Figure 6. Model of CREB3L1 protein interaction with DYNLL1. A single CREB3L1 TQT binding motif facilitates interactions with DYNLL1. This interaction may occur in the cytoplasm, where CREB3L1 appears to promote DYNLL1 nuclear translocation, as well as in the nucleus. In the nucleus, we propose that DYNLL1 functions like a molecular glue to assist CREB3L1 heterodimerisation with other proteins, with one candidate protein being CREB3 family member CREB3L2. This interaction serves to enhance the transcriptional activation of CREB3L1 target genes including *Avp*.

10. References

1. Honma Y, Kanazawa K, Mori T, Tanno Y, Tojo M, Kiyosawa H, et al. Identification of a novel gene, OASIS, which encodes for a putative CREB/ATF family transcription factor in the long-term cultured astrocytes and gliotic tissue. Brain Res Mol Brain Res. 1999;69(1):93-103.
2. Kondo S, Saito A, Asada R, Kanemoto S, Imaizumi K. Physiological unfolded protein response regulated by OASIS family members, transmembrane bZIP transcription factors. IUBMB Life. 2011;63(4):233-9.
3. Chan CP, Kok KH, Jin DY. CREB3 subfamily transcription factors are not created equal: Recent insights from global analyses and animal models. Cell Biosci. 2011;1(1):6.
4. Kondo S, Murakami T, Tatsumi K, Ogata M, Kanemoto S, Otori K, et al. OASIS, a CREB/ATF-family member, modulates UPR signalling in astrocytes. Nat Cell Biol. 2005;7(2):186-U12.
5. Murakami T, Kondo S, Ogata M, Kanemoto S, Saito A, Wanaka A, et al. Cleavage of the membrane-bound transcription factor OASIS in response to endoplasmic reticulum stress. J Neurochem. 2006;96(4):1090-100.
6. Murakami T, Saito A, Hino SI, Kondo S, Kanemoto S, Chihara K, et al. Signalling mediated by the endoplasmic reticulum stress transducer OASIS is involved in bone formation. Nat Cell Biol. 2009;11(10):1205-U90.
7. Omori Y, Imai JI, Suzuki Y, Watanabe S, Tanigami A, Sugano S. OASIS is a transcriptional activator of CREB/ATF family with a transmembrane domain. Biochem Bioph Res Co. 2002;293(1):470-7.
8. Zhao Y, Yu Z, Song Y, Fan L, Lei T, He Y, et al. The Regulatory Network of CREB3L1 and Its Roles in Physiological and Pathological Conditions. Int J Med Sci. 2024;21(1):123-36.
9. Sampieri L, Di Giusto P, Alvarez C. CREB3 Transcription Factors: ER-Golgi Stress Transducers as Hubs for Cellular Homeostasis. Front Cell Dev Biol. 2019;7.
10. Reinke AW, Baek J, Ashenberg O, Keating AE. Networks of bZIP Protein-Protein Interactions Diversified Over a Billion Years of Evolution. Science. 2013;340(6133):730-4.
11. Rodriguez-Martinez JA, Reinke AW, Bhimsaria D, Keating AE, Ansari AZ. Combinatorial bZIP dimers display complex DNA-binding specificity landscapes. Elife. 2017;6.
12. Greenwood M, Bordieri L, Greenwood MP, Melo MR, Colombari DSA, Colombari E, et al. Transcription Factor CREB3L1 Regulates Vasopressin Gene Expression in the Rat Hypothalamus. J Neurosci. 2014;34(11):3810-20.
13. Greenwood M, Gillard BT, Farrukh R, Paterson A, Althammer F, Grinevich V, et al. Transcription factor Creb3l1 maintains proteostasis in neuroendocrine cells. Mol Metab. 2022;63.
14. Greenwood M, Paterson A, Rahman PA, Gillard BT, Langley S, Iwasaki Y, et al. Transcription factor Creb3l1 regulates the synthesis of prohormone convertase enzyme PC1/3 in endocrine cells. J Neuroendocrinol. 2020;32(4).
15. Greenwood MP, Greenwood M, Gillard BT, Chitra Devi R, Murphy D. Regulation of cAMP Responsive Element Binding Protein 3-Like 1 (Creb3l1) Expression by Orphan Nuclear Receptor Nr4a1. Front Mol Neurosci. 2017;10:413.
16. Denard B, Lee C, Ye J. Doxorubicin blocks proliferation of cancer cells through proteolytic activation of CREB3L1. Elife. 2012;1.
17. Garcia IA, Torres Demichelis V, Viale DL, Di Giusto P, Ezhova Y, Polishchuk RS, et al. CREB3L1-mediated functional and structural adaptation of the secretory pathway in hormone-stimulated thyroid cells. J Cell Sci. 2017;130(24):4155-67.
18. Saito A, Kamikawa Y, Ito T, Matsuhisa K, Kaneko M, Okamoto T, et al. p53-independent tumor suppression by cell-cycle arrest via CREB/ATF transcription factor OASIS. Cell Rep. 2023;42(5).

19. Saito A, Kanemoto S, Kawasaki N, Asada R, Iwamoto H, Oki M, et al. Unfolded protein response, activated by OASIS family transcription factors, promotes astrocyte differentiation. Nat Commun. 2012;3.
20. Vellanki RN, Zhang L, Guney MA, Rocheleau JV, Gannon M, Volchuk A. OASIS/CREB3L1 induces expression of genes involved in extracellular matrix production but not classical endoplasmic reticulum stress response genes in pancreatic beta-cells. Endocrinology. 2010;151(9):4146-57.
21. Eleveld-Trancikova D, Sanecka A, van Hout-Kuijer MA, Looman MWG, Hendriks IAM, Jansen BJH, et al. DC-STAMP interacts with ER-resident transcription factor LUMAN which becomes activated during DC maturation. Mol Immunol. 2010;47(11-12):1963-73.
22. Freiman RN, Herr W. Viral mimicry: common mode of association with HCF by VP16 and the cellular protein LZIP. Genes Dev. 1997;11(23):3122-7.
23. Jin DY, Wang HL, Zhou Y, Chun AC, Kibler KV, Hou YD, et al. Hepatitis C virus core protein-induced loss of LZIP function correlates with cellular transformation. EMBO J. 2000;19(4):729-40.
24. Ko J, Jang SW, Kim YS, Kim IS, Sung HJ, Kim HH, et al. Human LZIP binds to CCR1 and differentially affects the chemotactic activities of CCR1-dependent chemokines. FASEB J. 2004;18(7):890-2.
25. Keller RB, Tran TT, Pyott SM, Pepin MG, Savarirayan R, McGillivray G, et al. Monoallelic and biallelic CREB3L1 variant causes mild and severe osteogenesis imperfecta, respectively. Genet Med. 2018;20(4):411-9.
26. Kamikawa Y, Saito A, Matsuhisa K, Kaneko M, Asada R, Horikoshi Y, et al. OASIS/CREB3L1 is a factor that responds to nuclear envelope stress. Cell Death Discov. 2021;7(1).
27. Greenwood M, Bordieri L, Greenwood MP, Rosso Melo M, Colombari DS, Colombari E, et al. Transcription factor CREB3L1 regulates vasopressin gene expression in the rat hypothalamus. J Neurosci. 2014;34(11):3810-20.
28. Greenwood M, Greenwood MP, Mecawi AS, Loh SY, Rodrigues JA, Paton JF, et al. Transcription factor CREB3L1 mediates cAMP and glucocorticoid regulation of arginine vasopressin gene transcription in the rat hypothalamus. Mol Brain. 2015;8(1):68.
29. Greenwood M, Greenwood MP, Paton JF, Murphy D. Transcription Factor CREB3L1 Regulates Endoplasmic Reticulum Stress Response Genes in the Osmotically Challenged Rat Hypothalamus. PLoS One. 2015;10(4):e0124956.
30. Greenwood M, Paterson A, Rahman PA, Gillard BT, Langley S, Iwasaki Y, et al. Transcription factor Creb3l1 regulates the synthesis of prohormone convertase enzyme PC1/3 in endocrine cells. J Neuroendocrinol. 2020;32(4):e12851.
31. Faul F, Erdfelder E, Buchner A, Lang AG. Statistical power analyses using G*Power 3.1: Tests for correlation and regression analyses. Behav Res Methods. 2009;41(4):1149-60.
32. Khongwichit S, Sornjai W, Jitobaom K, Greenwood M, Greenwood MP, Hitakarun A, et al. A functional interaction between GRP78 and Zika virus E protein. Sci Rep. 2021;11(1):393.
33. Greenwood MP, Greenwood M, Paton JF, Murphy D. Salt appetite is reduced by a single experience of drinking hypertonic saline in the adult rat. PLoS One. 2014;9(8):e104802.
34. Livak KJ, Schmittgen TD. Analysis of relative gene expression data using real-time quantitative PCR and the 2(T)(-Delta Delta C) method. Methods. 2001;25(4):402-8.
35. Greenwood M, Greenwood MP, Mecawi AS, Loh SY, Rodrigues JA, Paton JFR, et al. Transcription factor CREB3L1 mediates cAMP and glucocorticoid regulation of arginine vasopressin gene transcription in the rat hypothalamus. Mol Brain. 2015;8.
36. Sievers F, Wilm A, Dineen D, Gibson TJ, Karplus K, Li W, et al. Fast, scalable generation of high-quality protein multiple sequence alignments using Clustal Omega. Mol Syst Biol. 2011;7:539.
37. Rouillard AD, Gundersen GW, Fernandez NF, Wang ZC, Monteiro CD, McDermott MG, et al. The harmonizome: a collection of processed datasets gathered to serve and mine knowledge about genes and proteins. Database-Oxford. 2016.

38. Greenwood MP, Mecawi AS, Hoe SZ, Mustafa MR, Johnson KR, Al-Mahmoud GA, et al. A comparison of physiological and transcriptome responses to water deprivation and salt loading in the rat supraoptic nucleus. Am J Physiol-Reg I. 2015;308(7):R559-R68.
39. Kaiser FJ, Tavassoli K, Van den Bemd GJ, Chang GT, Horsthemke B, Moroy T, et al. Nuclear interaction of the dynein light chain LC8a with the TRPS1 transcription factor suppresses the transcriptional repression activity of TRPS1. Hum Mol Genet. 2003;12(11):1349-58.
40. Lajoix AD, Badiou S, Péraldi-Roux S, Chardès T, Dietz S, Aknin C, et al. Protein inhibitor of neuronal nitric oxide synthase (PIN) is a new regulator of glucose-induced insulin secretion. Diabetes. 2006;55(12):3279-88.
41. Rapali P, García-Mayoral MF, Martínez-Moreno M, Tárnok K, Schlett K, Albar JP, et al. LC8 dynein light chain (DYNLL1) binds to the C-terminal domain of ATM-interacting protein (ATMIN/ASCIZ) and regulates its subcellular localization. Biochem Bioph Res Co. 2011;414(3):493-8.
42. Rayala SK, den Hollander P, Balasenthil S, Yang ZB, Broaddus RR, Kumar R. Functional regulation of estrogen receptor pathway by the dynein light chain 1 (vol 6, pg 538, 2005). Embo Rep. 2005;6(11):1101-.
43. Cui M, Kanemoto S, Cui X, Kaneko M, Asada R, Matsuhisa K, et al. OASIS modulates hypoxia pathway activity to regulate bone angiogenesis. Sci Rep-Uk. 2015;5.
44. Jaffrey SR, Snyder SH. PIN: An associated protein inhibitor of neuronal nitric oxide synthase. Science. 1996;274(5288):774-7.
45. Yang JJ, Dennison NN, Reiss CS. PIN:: A novel protein involved in IFN-γ accumulation of NOS-1 in neurons. DNA Cell Biol. 2008;27(1):9-18.
46. Fang M, Jaffrey SR, Sawa A, Ye KQ, Luo XJ, Snyder SH. Dexras1: A G protein specifically coupled to neuronal nitric oxide synthase via CAPON. Neuron. 2000;28(1):183-93.
47. Pauza AG, Mecawi AS, Paterson A, Hindmarch CCT, Greenwood M, Murphy D, et al. Osmoregulation of the transcriptome of the hypothalamic supraoptic nucleus: A resource for the community. J Neuroendocrinol. 2021;33(8).
48. Rapali P, Radnai L, Süveges D, Harmat V, Tölgyesi F, Wahlgren WY, et al. Directed Evolution Reveals the Binding Motif Preference of the LC8/DYNLL Hub Protein and Predicts Large Numbers of Novel Binders in the Human Proteome. Plos One. 2011;6(4).
49. Herzig RP, Andersson U, Scarpulla RC. Dynein light chain interacts with NRF-1 and EWG, structurally and functionally related transcription factors from humans and drosophila. J Cell Sci. 2000;113 Pt 23:4263-73.
50. Kim H, Hyeon S, Kim H, Yang Y, Huh JY, Park DR, et al. Dynein light chain LC8 inhibits osteoclast differentiation and prevents bone loss in mice. J Immunol. 2013;190(3):1312-8.
51. Lo KWH, Kan HM, Chan LN, Xu WG, Wang KP, Wu ZG, et al. The 8-kDa dynein light chain binds to p53-binding protein 1 and mediates DNA damage-induced p53 nuclear accumulation. J Biol Chem. 2005;280(9):8172-9.
52. Vadlamudi RK, Bagheri-Yarmand R, Yang Z, Balasenthil S, Nguyen D, Sahin AA, et al. Dynein light chain 1, a p21-activated kinase 1-interacting substrate, promotes cancerous phenotypes. Cancer Cell. 2004;5(6):575-85.
53. Barbar E. Dynein light chain LC8 is a dimerization hub essential in diverse protein networks. Biochemistry. 2008;47(2):503-8.
54. Alcock F, Swanton E. Mammalian OS-9 Is Upregulated in Response to Endoplasmic Reticulum Stress and Facilitates Ubiquitination of Misfolded Glycoproteins. J Mol Biol. 2009;385(4):1032-42.
55. Otto H, Conz C, Maier P, Wölfle T, Suzuki CK, Jenö P, et al. The chaperones MPP11 and Hsp70L1 form the mammalian ribosome-associated complex. P Natl Acad Sci USA. 2005;102(29):10064-9.
56. Wu IH, Yoon JS, Yang Q, Liu Y, Skach W, Thomas P. A role for the ribosome-associated complex in activation of the IRE1 branch of UPR. Cell Rep. 2021;35(10).

57. Greenwood M, Greenwood MP, Paton JFR, Murphy D. Transcription Factor CREB3L1 Regulates Endoplasmic Reticulum Stress Response Genes in the Osmotically Challenged Rat Hypothalamus. Plos One. 2015;10(4).
58. Luo H, Jiang M, Lian GL, Liu Q, Shi M, Li TY, et al. AIDA Selectively Mediates Downregulation of Fat Synthesis Enzymes by ERAD to Retard Intestinal Fat Absorption and Prevent Obesity. Cell Metab. 2018;27(4):843-+.
59. Suyama S, Kodaira-Hirano M, Otgon-Uul Z, Ueta Y, Nakata M, Yada T. Fasted/fed states regulate postsynaptic hub protein DYNLL2 and glutamatergic transmission in oxytocin neurons in the hypothalamic paraventricular nucleus. Neuropeptides. 2016;56:115-23.

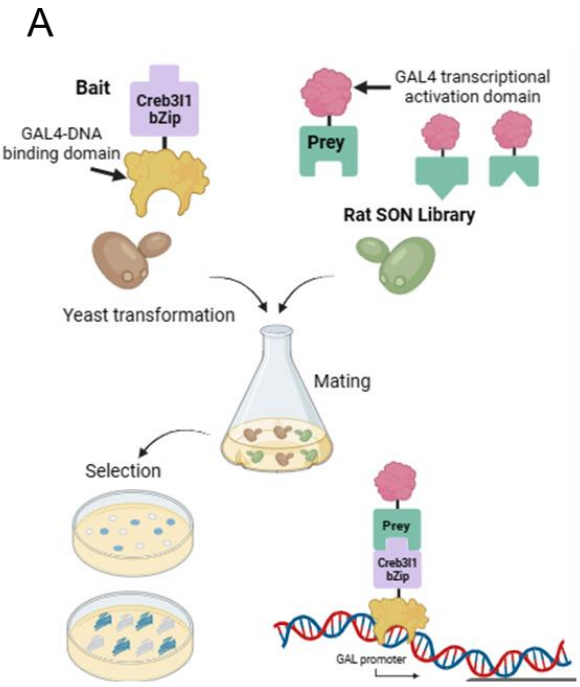

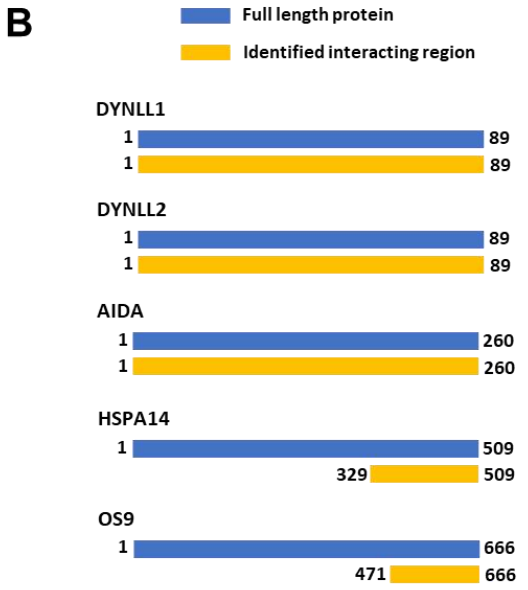

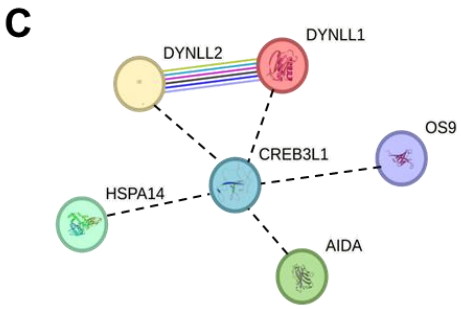

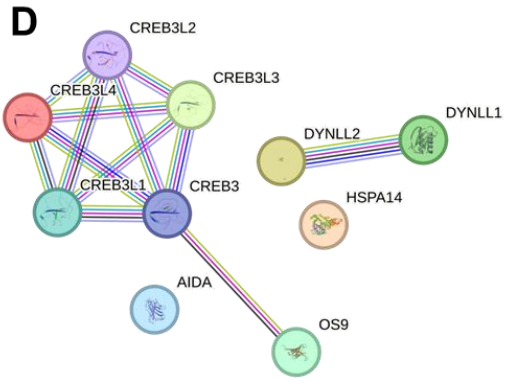

E

CREB3L1 TQT motifs

```
Mouse_CREB3L1      PYKMAATQTG
Human_CREB3L1      PYKMAATQTG
Rat_CREB3L1        PYKMAATQTG
                   **********
```

F

CREB3 family TQT motifs

```
Rat_CREB3L1        PYKMAATQTG
Mouse_CREB3L2      TCKLAGTQTG
Human_CREB3L2      TCKLAGTQTG
Rat_CREB3L2        TCKLAGTQTG
                     :*:.****
```

Fig. 1

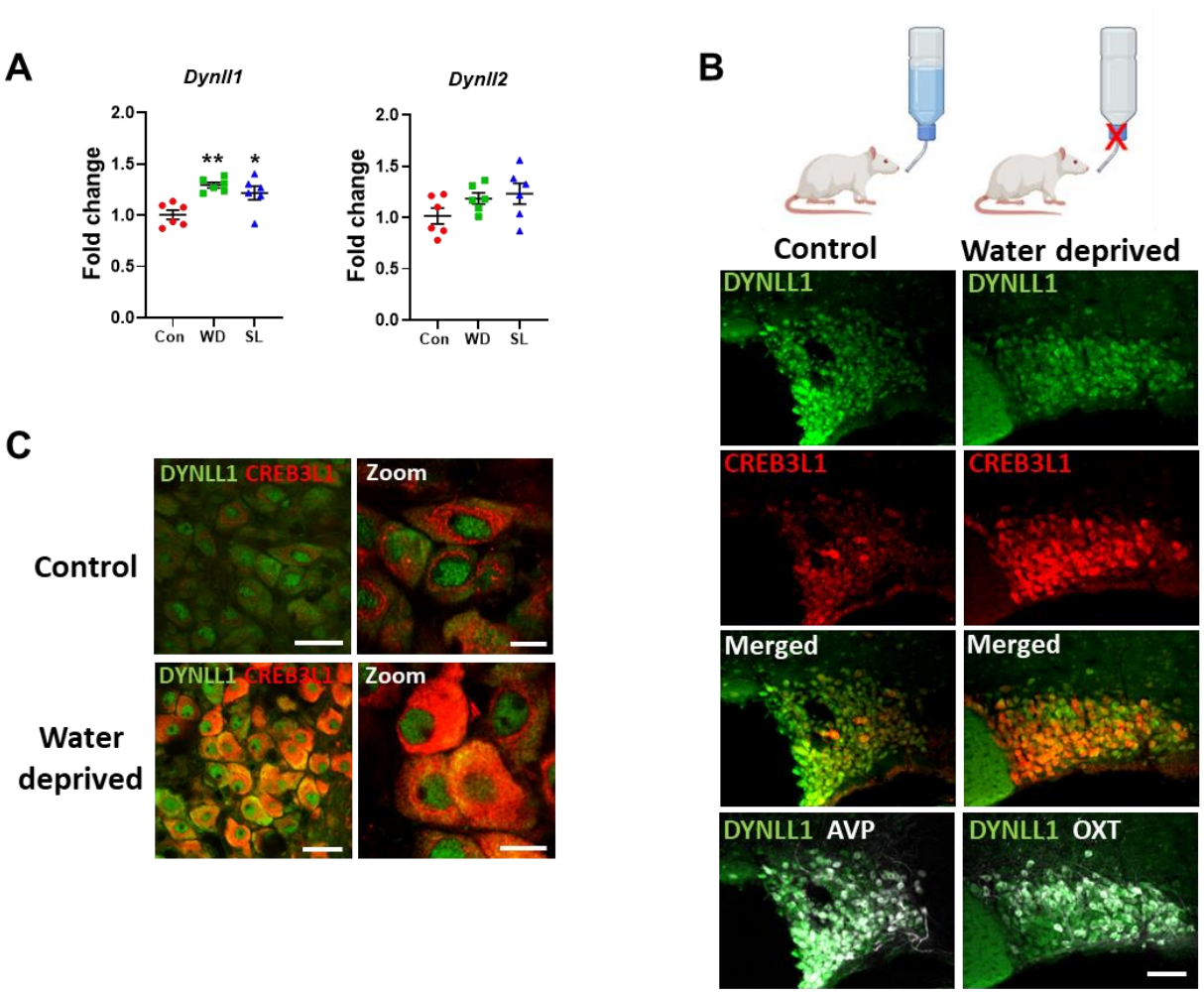
A
Dynll1
Dynll2
Fold change
2.0
1.5
1.0
0.5
0.0
**
*
Con
WD
SL
B
Control
Water deprived
DYNLL1
CREB3L1
Merged
DYNLL1 AVP
DYNLL1 OXT
C
Control
Water deprived
DYNLL1 CREB3L1
Zoom

Fig. 2

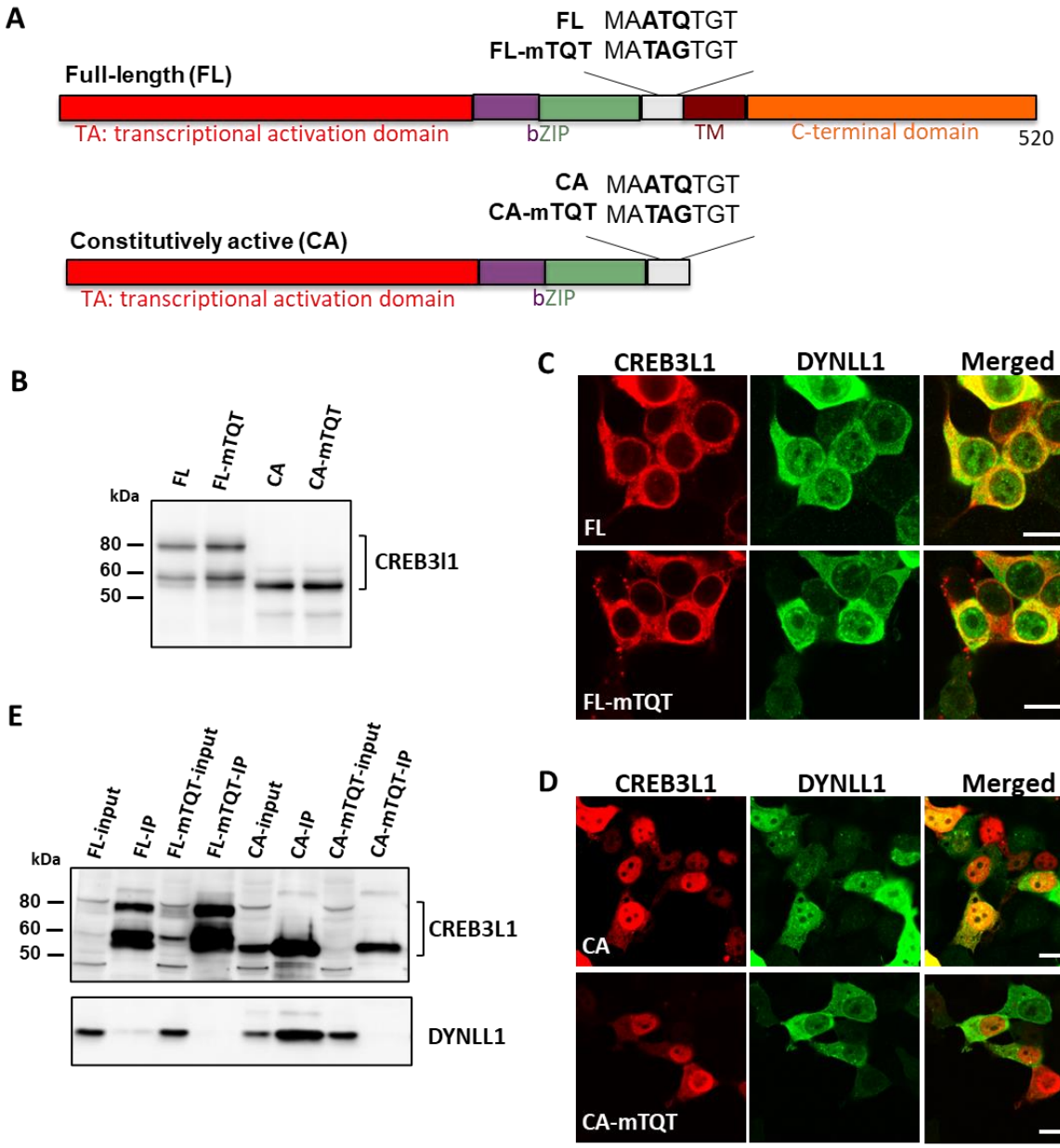
A
FL MAATQTGT
FL-mTQT MATAGTGT
Full-length (FL)
TA: transcriptional activation domain
bZIP
TM
C-terminal domain
520
CA MAATQTGT
CA-mTQT MATAGTGT
Constitutively active (CA)
TA: transcriptional activation domain
bZIP
B
FL
FL-mTQT
CA
CA-mTQT
kDa
80
60
50
CREB3l1
C
CREB3L1
DYNLL1
Merged
FL
FL-mTQT
D
CREB3L1
DYNLL1
Merged
CA
CA-mTQT
E
FL-input
FL-IP
FL-mTQT-input
FL-mTQT-IP
CA-input
CA-IP
CA-mTQT-input
CA-mTQT-IP
kDa
80
60
50
CREB3L1
DYNLL1

Fig. 3

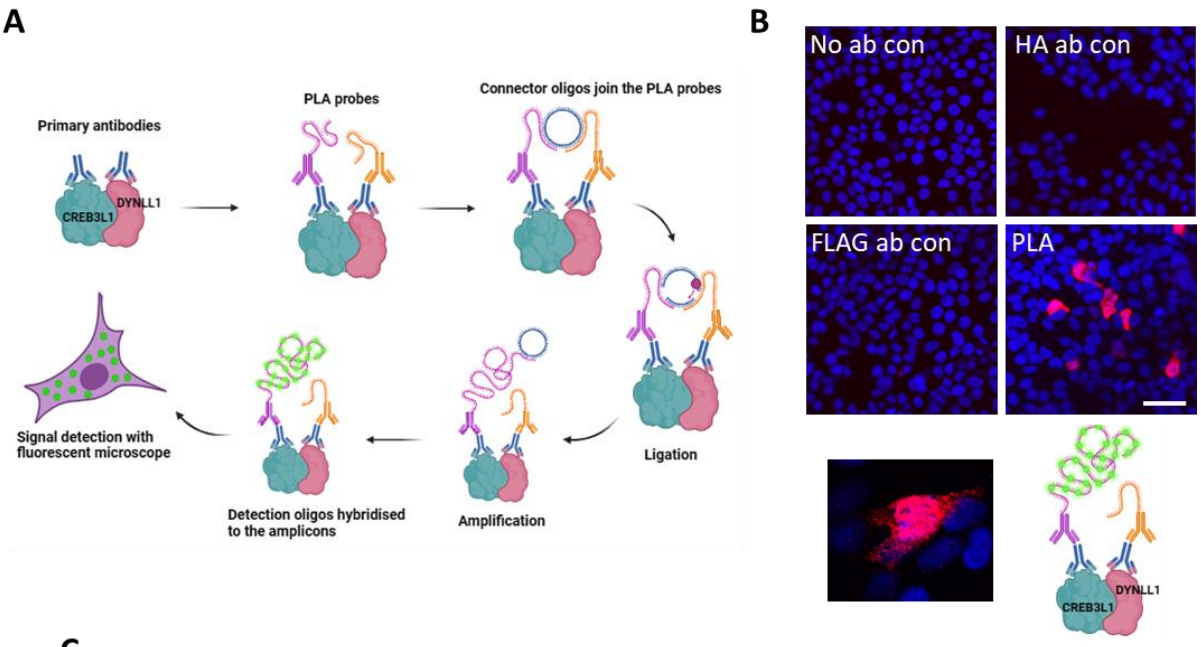
A
Primary antibodies
CREB3L1
DYNLL1
PLA probes
Connector oligos join the PLA probes
Ligation
Amplification
Detection oligos hybridised to the amplicons
Signal detection with fluorescent microscope
B
No ab con
HA ab con
FLAG ab con
PLA
DYNLL1
CREB3L1
C
DMSO
FSK
DYNLL1
DYNLL1
DYNLL1 CREB3L1
DYNLL1 CREB3L1
D
pcDNA
Dynll1
DMSO
FSK
DMSO
FSK
In
IP
In
IP
In
IP
In
IP
kDa
80
60
50
E
CREB3L1 ab con
HA ab con
DMSO - PLA
FSK - PLA

Fig. 4

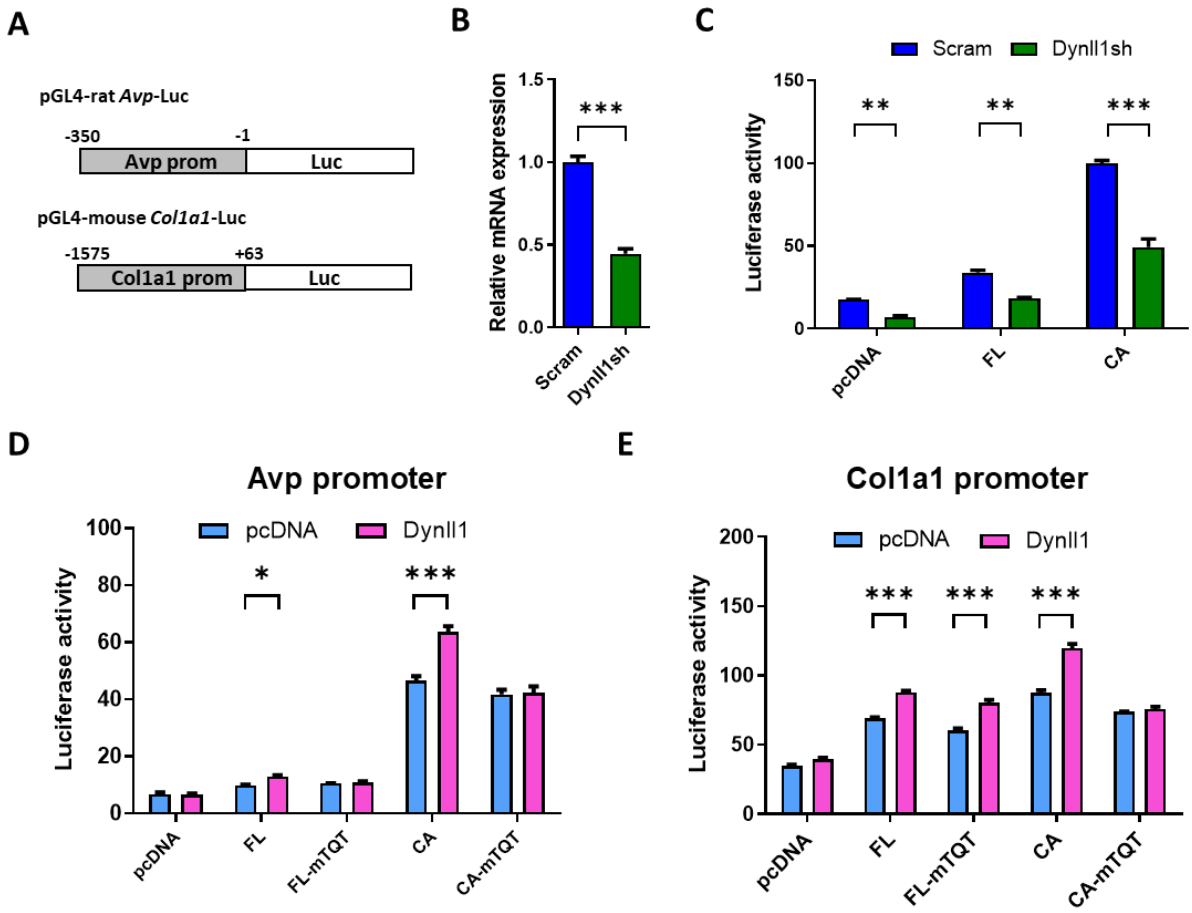
A
pGL4-rat Avp-Luc
-350
-1
Avp prom
Luc
pGL4-mouse Col1a1-Luc
-1575
+63
Col1a1 prom
Luc
B
Relative mRNA expression
1.5
1.0
0.5
0.0
***
Scram
Dynll1sh
C
Scram
Dynll1sh
Luciferase activity
150
100
50
0
**
**
***
pcDNA
FL
CA
D
Avp promoter
pcDNA
Dynll1
Luciferase activity
100
80
60
40
20
0
*
***
pcDNA
FL
FL-mTQT
CA
CA-mTQT
E
Col1a1 promoter
pcDNA
Dynll1
Luciferase activity
200
150
100
50
0
***
***
***
pcDNA
FL
FL-mTQT
CA
CA-mTQT

Fig. 5

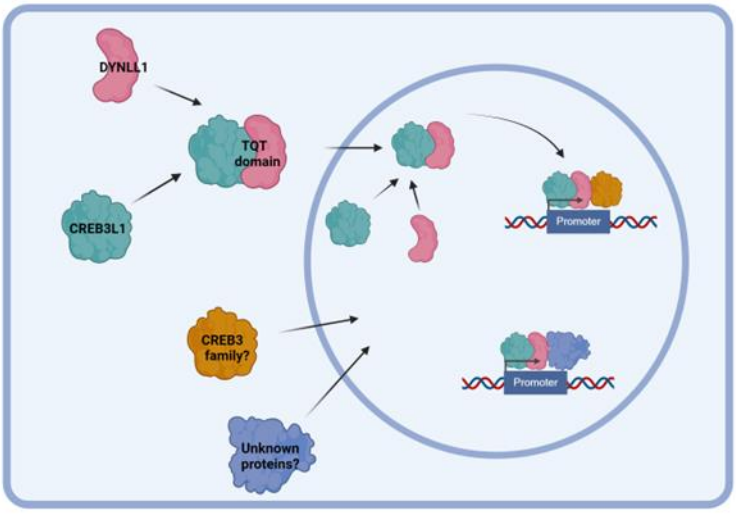
DYNLL1
TQT domain
CREB3L1
CREB3 family?
Unknown proteins?
Promoter
Promoter

Fig. 6.